Journal of Sound and Vibration (1999) **219**(1), 5–22
Article No. jsvi.1998.1821, available online at http://www.idealibrary.com.on IDEAL

DEVELOPMENT OF THE EXPERIMENTAL SPATIAL MATRIX IDENTIFICATION METHOD (THEORY AND BASIC VERIFICATION WITH A FRAME STRUCTURE)

M. Okuma, Q. Shi and T. Oho

Department of Mechanical Engineering and Science,
Tokyo Institute of Technology, 2-12-1, *O-okayama*, *Meguro-ku*, *Tokyo*, *Japan*

(*Received* 16 *April* 1997, *and in final form* 28 *May* 1998)

In the present paper, the authors propose a new experimental method of identifying the set of spatial matrices. This method identifies the spatial matrices, namely mass matrix, damping matrix and stiffness matrix, which describe the properties of dynamic structures, using experimentally measured FRFs (Frequency Response Functions) within the frequency range of interest. In this paper, the theory developed for this method is introduced. The validity of the proposed method is verified by its application to an actual frame structure using experimental FRFs measured by hammering tests.

1. INTRODUCTION

In general, mechanical vibration analysis begins with the formulation of the equations of motion in the physical domain. For example, the equations of motion are expressed as equation (1) by assuming viscous damping:

$$[\mathbf{M}]\{\ddot{\boldsymbol{x}}(t)\} + [\mathbf{C}]\{\dot{\boldsymbol{x}}(t)\} + [\mathbf{K}]\{\boldsymbol{x}(t)\} = \{\boldsymbol{f}(t)\}, \tag{1}$$

where [**M**] is the mass matrix of the objective structure, [**C**] is the viscous damping matrix, [**K**] is the stiffness matrix, $\{\boldsymbol{x}(t)\}$ is the displacement response vector with $\{\dot{\boldsymbol{x}}\}$ and $\{\ddot{\boldsymbol{x}}\}$ representing its velocity and acceleration, and $\{\boldsymbol{f}(t)\}$ is the applied external force vector.

The mass matrix, the damping matrix and the stiffness matrix are called spatial matrices because they are formulated in the physical domain. If spatial matrices are accurately obtained, it is possible to perform any kind of vibration and design analysis successfully. For example, it is quite easy to obtain the modal parameters from the spatial matrices by the numerical methods presently available for eigenvalue problems.

The spatial matrices can be theoretically formulated. The most primitive method for this formulation would be the manual formulation for mass–spring systems. A more sophisticated example would be the finite element method. Such theoretical approaches have the advantage that they can be carried out without

0022–460X/99/010005 + 18 $30.00/0

using actual objective structures. However, it is often impractical to theoretically formulate accurate spatial matrices of actual mechanical structures due to structure complexity. Therefore, experimental approaches are desirable from a practical viewpoint. If spatial matrices can be experimentally as well as theoretically formulated for any complex structure, it becomes much easier to link experimental approaches to theoretical ones in MCAE (Mechanical Computer Aided Engineering). To the authors' knowledge, however, it is generally considered difficult to identify spatial matrices representing the high frequency dynamic characteristics of structures from experimental FRFs (Frequency Response Functions). Instead of spatial matrices, modal parameters, such as natural frequencies and natural modes, are the parameters generally identified from experimental FRFs. Many methods [1] have already been proposed to identify modal parameters, and are widely used as basic tools for vibration analysis. In order to link the experimental modal parameters to spatial matrices for MCAE vibration analysis, a number of additional mathematical operations, some possibly complex, may be required. The methods of experimentally identifying spatial matrices have been proposed by Leuridan [2], Roemer [3], Minas [4], Peterson [5], Okuma [6] and others. However, unfortunately, many of these methods have not been developed to the point that they can be experimentally applied. The authors believe that the spatial matrices to be identified experimentally must be subject to the following conditions from the practical viewpoint of structural vibration analysis:

(1) It must be possible to set the number of degrees of freedom of spatial matrices to a value much larger than the number of resonant frequencies located inside the frequency range of interest.
(2) The spatial matrices identified must be able to represent the dynamic characteristics of the structure under arbitrary boundary conditions, even conditions that differ from those in place at the time of the identification.

The first condition is introduced in order to meet the requirement for the adequate number of degrees of spatial freedom necessary for structural vibration analysis. The second condition implies the practical use of the spatial matrices for such processes as structural modification, optimum design, and vibration control. In this paper, a method is presented for identifying spatial matrices that satisfactorily meets both the above conditions.

In the following section, the theory and the procedure of the method are explained. In the third section, as an application, spatial matrices are identified from the FRFs experimentally measured at 22 points to represent an actual frame structure under the free–free boundary condition. Finally, some basic investigations of spatial matrices are discussed in order to demonstrate the validity and the usefulness of the method for practical applications.

2. THEORY

Figure 1 shows a flow-chart of the proposed identification method. It is assumed here that a structure to be identified is under the free–free boundary condition for

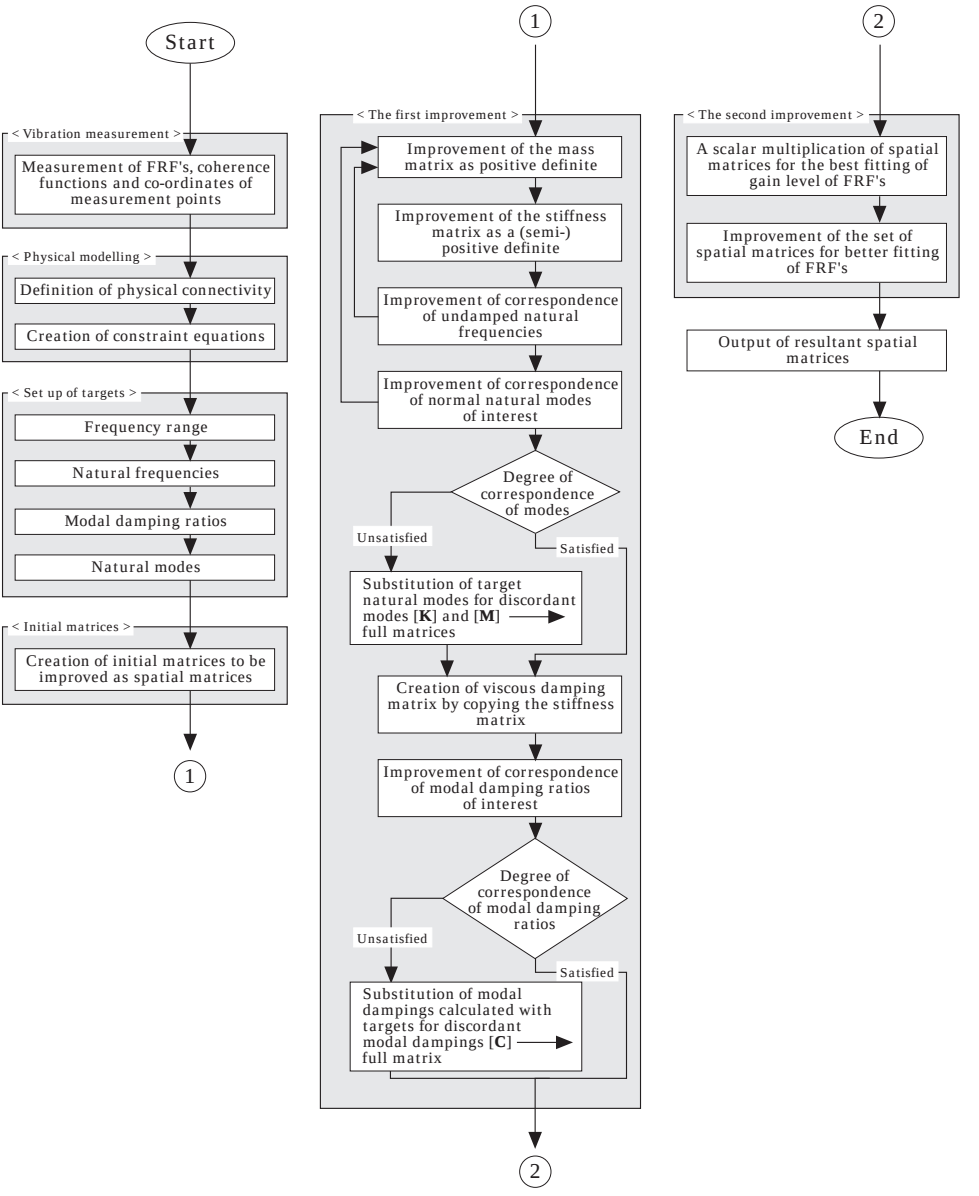

Figure 1. Flow-chart of the theory.

vibration testing. Rubber strings or other elastic devices of small mass are expected to be the most useful for suspending the structure.

First, the FRFs and their associating coherence functions are measured at the chosen measurement points, and the co-ordinates of the measurement points must be expressed in terms of a defined co-ordinate system. These two sets of data, the experimental FRFs and the measurement point co-ordinates, are the essential inputs for the identification method. The number of measurement points should be adequate to depict the shapes of the resonant vibration modes existing in the identification frequency range. External force should be applied at an appropriate

point of the test structure such that all feasible rigid motions may be excited simultaneously.

The process of "physical modelling" consists of creating physical connectivity among the measurement points in order to define the structural direct connectivity among them. This preparation method is similar to the method of defining connectivity using elements of the finite element method. It is also very similar to the preparation method of setting contour lines for displaying mode animation by experimental modal parameter estimation programs. According to the connectivity, this last method can automatically determine the physical connection, such as which elements are necessarily set as zero-elements in the spatial matrices. Then, the constraint equations among the other elements can be formulated based on the following principle. The mass matrix of any system having multi degrees of freedom must be defined by

$$[\boldsymbol{\psi}]^{\mathrm{T}}[\mathbf{M}][\boldsymbol{\psi}] = [\mathbf{M}_{rigid}], \tag{2}$$

where $[\boldsymbol{\psi}]$ is the matrix of mutually independent rigid motion modes, $[\mathbf{M}]$ is the mass matrix to be identified, and $[\mathbf{M}_{rigid}]$ is a rigid body mass matrix.

It is well known that $[\boldsymbol{\psi}]$ can be formulated with the co-ordinates of the measurement points. The proper formation of any rigid body mass matrix is well known.

$$[\mathbf{M}_{rigid}] = \begin{bmatrix} m & & & & & \\ 0 & m & & & sym. & \\ 0 & 0 & m & & & \\ 0 & -C & B & I_{xx} & & \\ C & 0 & -A & I_{yx} & I_{yy} & \\ -B & A & 0 & I_{zx} & I_{zy} & I_{zz} \end{bmatrix}, \tag{3}$$

where m is the mass of the structure; I_{xx}, I_{yy}, I_{zz} are inertia of moment around x-axis, y-axis and z-axis respectively; I_{yx}, I_{zx}, I_{zy} are products of the moment inertia; (x_g, y_g, z_g) is the co-ordinate of the center of gravity of the structure; and A, B, C are parameters based on the relations: $A = mx_g$, $B = my_g$, $C = mz_g$.

As a result, even without knowing the rigid body properties of the structure, several constraint equations among the elements of the mass matrix $[\mathbf{M}]$ can be created by equation (2). Namely, some elements are expressed as dependent variables by the linear combination of the other elements, which are dealt with as independent variables, by the constraint equations. Furthermore, if some of the rigid body properties are known, for example the mass of the structure, it is possible to use the known values to create the constraint equations.

With respect to the stiffness matrix, the following equation can be formulated according to the principle that no stress appears at any point of the structure for any feasible rigid body motion:

$$[\mathbf{K}][\boldsymbol{\psi}] = [\mathbf{0}], \tag{4}$$

where $[\mathbf{K}]$ is the stiffness matrix to be identified, and $[\mathbf{0}]$ is a zero element matrix.

Consequently, several constraint equations can also be created from equation (4). And the constraint equations regarding the viscous damping matrix can be created based on the identical concept of the stiffness matrix as well.

In the process of setting up the targets, one first sets up the frequency range for identification. The lower boundary frequency must be set at a value below the first resonant frequency of the structure based on observing the accuracy of the phases, coherence functions, and other attributes of the FRFs. The lower the frequency is set, the better will be the expected accuracy. The upper boundary frequency may be set at a high value, provided that the shapes of all natural modes existing in the identification frequency range can be distinguished clearly by depiction with measurement points. After that, one identifies the natural frequencies, the natural modes and the associating modal damping ratios in the identification frequency range. Any modal parameter estimation method [1, 7] can be used for this procedure. Hereafter, the modal parameters are referred to as "targets".

In the process of "defining the initial matrices", the initial matrices have to be set to begin the identification because of the iterative nature of the method. The initial elements of the mass matrix and the stiffness matrix are set up by substituting random numbers into the independent variables of the constraint equations. This method is fast and simple, and no better way to set up the initial matrices has yet been found.

In the process of "defining the first improvement", the initial mass matrix is improved to become a positive definite matrix. The mass matrix is normalized by the biggest absolute value of the elements. Then, the eigenvalues are calculated

$$[\mathbf{M}]\{\boldsymbol{\phi}\} = \lambda\{\boldsymbol{\phi}\}. \tag{5}$$

If any of the eigenvalues of equation (5) is negative, the matrix is judged as definitively negative. Then, the first order differentials of the negative eigenvalues with respect to the independent variables are computed by (reference [8]):

$$\partial\lambda/\partial m_{ij} = \{\boldsymbol{\phi}\}^{\mathrm{T}}(\partial[\mathbf{M}]/\partial m_{ij})\{\boldsymbol{\phi}\}/\{\boldsymbol{\phi}\}^{\mathrm{T}}\{\boldsymbol{\phi}\}, \tag{6}$$

where m_{ij} is the element of mass matrix of row i and column j. The sensitivity analysis using only these differentials cannot transform the negative eigenvalues into positive ones rapidly, and thus, some other sensitivity equations must be added to them. The additional sensitivity equations are formulated with the differentials of the diagonal elements and the off-diagonal elements in order to move them toward the value of one and zero respectively. These additional equations work effectively to accelerate the movement of the initially negative eigenvalues to positive eigenvalues. The differentials of both diagonal and off-diagonal elements can be obtained as follows. Since all diagonal elements are always dealt with as dependent variables in the constraint equations, the coefficients of independent variables in the linear combinations can be taken as simply the differentials of the diagonal elements with respect to the independent variables. The differentials of the off-diagonal elements as dependent variables can also be expressed by the coefficients of independent variables in the constraint equations. It is clear that the differentials of off-diagonal elements as independent

variables all have the unit value of one. The aforementioned normalization is carried out at every iterative step of the sensitivity analysis.

The initial stiffness matrix is improved to become a semi-positive definite matrix by the above method. The eigenvalues calculated by equation (7) are controlled. It is noted here that the constraint equations of the physical modelling have necessarily set the differentials of the eigenvalues corresponding to the feasible rigid body natural motion modes to a value zero in advance.

$$[\mathbf{K}]\{\boldsymbol{\phi}\} = \lambda\{\boldsymbol{\phi}\}. \tag{7}$$

After this operation, some undamped first order natural frequencies obtained by the use of equation (8) are suited to fit well into the natural frequencies actually located in the identified frequency range by the sensitivity based analysis.

$$([\mathbf{K}] - \Omega^2[\mathbf{M}])\{\boldsymbol{\phi}\} = \{\mathbf{0}\}. \tag{8}$$

The sensitivities appearing in reference [8] of the rth order eigenvalue with respect to independent variables of the stiffness matrix and the mass matrix can be computed by equations (9) and (10), which are derived from equation (8), respectively:

$$\partial\Omega_r^2/\partial k_{ij} = \{\boldsymbol{\phi}_r\}^{\mathrm{T}} \frac{\partial[\mathbf{K}]}{\partial k_{ij}} \{\boldsymbol{\phi}_r\}/\{\boldsymbol{\phi}_r\}^{\mathrm{T}}[\mathbf{M}]\{\boldsymbol{\phi}_r\},$$

$$\partial\Omega_r^2/\partial m_{ij} = -\lambda_r\{\boldsymbol{\phi}_r\}^{\mathrm{T}} \frac{\partial[\mathbf{M}]}{\partial m_{ij}} \{\boldsymbol{\phi}_r\}/\{\boldsymbol{\phi}_r\}^{\mathrm{T}}[\mathbf{M}]\{\boldsymbol{\phi}_r\}, \tag{9, 10}$$

where $\{\boldsymbol{\phi}_r\}$ is the rth eigenvector, Ω_r is the rth natural frequency, and λ_r is the rth eigenvalue. The natural frequencies located in the identification frequency range must be satisfactorily controlled. If they are not, the modelling is judged to be unacceptable and an improvement of the physical modelling, i.e., of the connectivity definition among the measurement points, is required. When the correspondence of the natural frequencies is satisfied, their associating natural modes are improved to correspond with the target modes by the sensitivity analysis of natural modes with respect to the independent variables of the stiffness and mass matrices. The sensitivities of the rth natural mode with respect to an element of the stiffness and the mass matrices are computed by equations (11) and (12), respectively:

$$\partial\{\boldsymbol{\phi}_r\}/\partial k_{ij} = [\boldsymbol{\Phi}]\{\boldsymbol{\eta}\}, \tag{11}$$

where k_{ij} is the element of stiffness matrix of row i and column j, $[\boldsymbol{\Phi}]$ is the eigenvector matrix, and $\{\boldsymbol{\eta}\}$ is the linear combinatioin coefficient vector whose elements can be calculated by,

$$\eta_p = -\{\boldsymbol{\phi}_p\}^{\mathrm{T}}(\partial[\mathbf{K}]/\partial k_{ij})\{\boldsymbol{\phi}_r\}/\Omega_p^2 - \Omega_r^2 (p \neq r),$$

$$\eta_r = 0, \tag{12}$$

$$\partial\{\boldsymbol{\phi}_r\}/\partial m_{ij} = [\boldsymbol{\Phi}]\{\boldsymbol{\eta}\}, \tag{13}$$

where m_{ij} is the element of mass matrix of row i and column j, while the elements of $\{\boldsymbol{\eta}\}$ can be calculated as

$$\eta_p = \lambda_r \{\boldsymbol{\phi}_p\}^{\mathrm{T}} (\partial[\mathbf{M}]/\partial m_{ij}) \{\boldsymbol{\phi}_r\} / (\Omega_p^2 - \Omega_r^2) (p \neq r),$$

$$\eta_r = -\tfrac{1}{2} \{\boldsymbol{\phi}_r\}^{\mathrm{T}} (\partial[\mathbf{M}]/\partial m_{ij}) \{\boldsymbol{\phi}_r\}, \tag{14}$$

When both the natural frequencies and the natural modes of interest are controlled satisfactorily, one proceeds to the process for determining the viscous damping matrix. Otherwise, the unsatisfactory natural modes calculated by equation (8) are coercively replaced by their target vectors normalized with respect to the mass matrix. One denotes the resultant modified natural mode matrix by $[\boldsymbol{\Phi}']$ here. Then, the mass matrix and the stiffness matrix are modified by;

$$[\mathbf{M}] = ([\boldsymbol{\Phi}']^{\mathrm{T}})^{-1} [\mathbf{I}] [\boldsymbol{\Phi}']^{-1}, \qquad [\mathbf{K}] = ([\boldsymbol{\Phi}']^{\mathrm{T}})^{-1} [\boldsymbol{\Omega}^2] [\boldsymbol{\Phi}']^{-1} \tag{15}$$

where $[\mathbf{I}]$ is an identity matrix, and $[\boldsymbol{\Omega}^2]$ is the diagonal matrix of eigenvalues. Note that both matrices become full element matrices.

The process for determining the viscous damping matrix is considered. At first, the initial viscous damping matrix is created by copying the resultant stiffness matrix. Then, the matrix is multiplied by a scalar value. The value is denoted as α, which is the proportional coefficient of the viscous damping matrix to the stiffness matrix. The modal damping ratio of the rth natural mode can be computed from the resultant spatial matrices. Under the normalization of the natural modes with respect to the mass matrix, the rth modal damping ratio ζ_r is defined with the undamped natural frequency Ω_r as expressed by:

$$\zeta_r = \tfrac{1}{2} \alpha \Omega_r. \tag{16}$$

The target modal damping ratios of the natural modes located in the identification frequency range have already been estimated in the process of setting up the targets. Therefore, by substituting the target modal damping ratios into equation (16), the most suitable value for the proportional coefficient α can be determined by the least mean squares method.

Furthermore, by conducting the sensitivity analysis of the eigenvalues with respect to the independent variables of the viscous damping, the viscous damping matrix is improved to make the modal damping ratios correspond better with the target values, provided that the natural modes obtained by equation (17) continue to correspond well with the natural modes already obtained by equation (8).

$$([\mathbf{C}] - \lambda_r [\mathbf{M}]) \{\boldsymbol{\phi}_r\} = \{\mathbf{0}\}. \tag{17}$$

Equation (17) implies that eigenvalues beginning with the smallest positive one should be controlled to correspond with the values defined by:

$$\lambda_r = 2\zeta_r \Omega_r (r = 1\text{–}n), \tag{17}$$

where λ_r is the rth eigenvalue to be derived from equation (17), ζ_r is the target modal damping ratio of the rth natural mode, Ω_r is the target natural frequency of the rth order, and n is the number of resonant vibration modes actually located in the identified frequency range.

When this control can be achieved, one advances to the last process. When control cannot be achieved, the unsatisfactory eigenvalues to be controlled are replaced by the values themselves as calculated by equation (18). Therefore, the viscous damping matrix is formulated by

$$[\mathbf{C}] = ([\mathbf{\Phi}']^{\mathrm{T}})^{-1}[\mathbf{\Lambda}][\mathbf{\Phi}']^{-1}, \tag{19}$$

where $[\mathbf{\Lambda}]$ is a diagonal matrix the elements of which are solved by equation (18). The matrix becomes a full element matrix and the resultant damping matrix becomes non-proportional to both the stiffness and mass matrices.

Finally, one moves to the last process referred to as the second improvement in Figure 1. Since the spatial matrices are computed basically under the treatment of the normalization mentioned above, there is no guarantee that the gain of the FRFs will correspond to that of the experimental FRFs after the previous processes. Consequently, the best scalar value should be determined by the least mean squares method in order that the gain of the FRFs fits well with the experimental FRFs. The value should be multiplied by the stiffness, mass, and damping matrices. Furthermore, the spatial matrices are improved in order to better fit the FRFs computed from the equations of motion to the experimental FRFs by a mathematical optimization method. The objective function to be minimized, subject to the physical modelling constraint equations mentioned above is:

$$J = \sum_{i=1}^{p} \{\Delta \boldsymbol{h}(\omega_i)\}^{\mathrm{H}}[\mathbf{W}(\omega_i)]\{\Delta \boldsymbol{h}(\omega_i)\} \tag{20}$$

where p is the number of sampling frequencies in the identification range, $\{\Delta \boldsymbol{h}(\omega_i)\}$ is the difference vector between experimental FRFs and the FRFs calculated with spatial matrices, H is symbol of the conjugate transpose, $[\mathbf{W}(\omega_i)]$ is the weighting function (a diagonal matrix), which are derived from coherence functions and FRFs based on the theory of the statistical likelihood estimation [9], and ω_i is the frequency.

A modified steepest descent method, explained below, is used. According to the authors' examinations of the identification by its application to some kinds of actual structures, quite large variances are observed among the sensitivities of the objective function, equation (20), with respect to the elements of the stiffness, mass and damping matrices. The spatial matrices having comparatively very small sensitivities cannot change at all by a steepest descent method that handles the independent variables of all spatial matrices simultaneously. Even after many iterations, the objective function does not decrease very substantially by this orthodox method. Nevertheless, the objective function may reduce more by an optimization method that partially selects the elements of the matrices as variables in every iterative process. That is to say, only the elements of the stiffness matrix are dealt with as variables in an iterative process. In the next iterative process, only the elements of the mass matrix are treated as variables. And in the still next iterative process, only the elements of the damping matrix are dealt with as variables. Finally, in the next process, all spatial matrices are handled

simultaneously. The various ways of handling the variables are repeated one after another in turns until the objective function converges. The results of this process are demonstrated by the practical application in section 3.

It should also be noted that the resultant spatial matrices are not the unique solution of the structure to be identified because this is a system identification which basically uses only experimental FRFs of a single point excitation and a limited identification frequency range. However, the resultant spatial matrices can represent the dynamic characteristics of the structure in the identification frequency range even in the case of changed boundary conditions and/or connection of some additional masses and stiffeners to this structure. Therefore, the spatial matrices can be used for many kinds of practical analyses.

3. BASIC VERIFICATION: AN EXPERIMENTAL APPLICATION

To show the practical validity of this method, a set of spatial matrices of an actual frame structure is identified, along with its FRFs, which are obtained by hammering tests.

Figure 2 illustrates a schematic view of the frame structure, which is constituted with L-shaped cross-sectional steel components. The structure is suspended by four rubber strings to simulate the free–free boundary condition on vibration testing. The origin of the co-ordinate system is placed at measurement point 12. The x-axis and y-axis are set vertically and horizontally, respectively. The z-axis is set with the right hand thumb rule as shown in Figure 2. Only the z-axial FRFs between the single point excitation at measurement point 1 and the multi-point responses at all 22 measurement points (1–22) are measured by hammering tests. The vibration responses are measured with a small accelerometer.

The dotted line in Figure 3 shows one of the experimental FRFs used as the input data for identification. The lower boundary frequency of the identification frequency range is set at 10 Hz due to the very low accuracy of the experimental FRFs below it. On the other hand, the upper boundary frequency is set at 180 Hz. The first four resonant vibration modes below 180 Hz are observed for the first torsional mode, the first bending mode, the second torsional mode and the second bending mode in ascending order of frequency as shown in Figure 4. The resonant frequencies of these modes are about 14, 86, 115 and 177 Hz, respectively. The number of measurement points lining up along the direction of the x-axis is 11 and it can be judged that these four resonant modes can be well distinguished by these 22 measurement points. This is the reason why 180 Hz was chosen as the upper boundary frequency here, although it should be noted that there are many other frequencies that might feasibly have been used. According to the actual frame structure, connectivity data among those 22 measurement points can be created to form a feasible physical modelling, and spatial matrices with 22 degrees of freedom are to be identified.

The accuracy of fitting FRFs of one of the measurement points is illustrated in Figure 3, in which the solid line denotes the FRFs calculated from the identified spatial matrices, and the results show that the identified FRFs are consistent with the experimental data. The FRFs of other measurement points calculated from the

identified spatial matrices also fit those of the experiment, as shown in Figure 3. The fitness of FRFs may be the most basic indicator for evaluation of the validity of the identification. It is also verified that the mode shapes calculated using the identified spatial matrices from the first to the fourth correspond very well with those obtained from the experimental FRFs by modal identification algorithm.

Table 1 lists all natural frequencies and the modal damping ratios calculated from the identified spatial matrices. The modelling of the vibration when considered only in the z-axial direction involves three feasible natural rigid motion modes. Therefore, the first three natural frequencies are 0 Hz, and the associating damping ratios are also zero. The next four natural frequencies show the resonances of the FRFs in the identified frequency range. The results show that the proposed method can control all residual natural frequencies located at higher frequencies than the identified frequency range. This control thus constitutes an essential function of the method, as explained in the previous section.

As one step in the verification of this method, the FRFs based prediction of locations that are not used in the identification is carried out with the identified spatial matrices. Figure 5 shows the comparison of FRFs between the measurement points 11 and 14 as one of the results. In the figure, the solid line denotes the predicted FRFs from the identified spatial matrices, and the dotted line indicates the experimental FRFs measured later for verification. The above results indicate that the prediction has an acceptable accuracy for this real application.

The next part of the investigation of the validity concerns the prediction accuracy of the structure under changing boundary conditions. FRFs of the structure defined by clamping four measurement points, 10, 11, 21 and 22, are calculated from the identified spatial matrices under the free–free boundary condition by simply deleting the four degrees of freedom corresponding to those four measurement points in the spatial matrices. Figure 6 shows the prediction

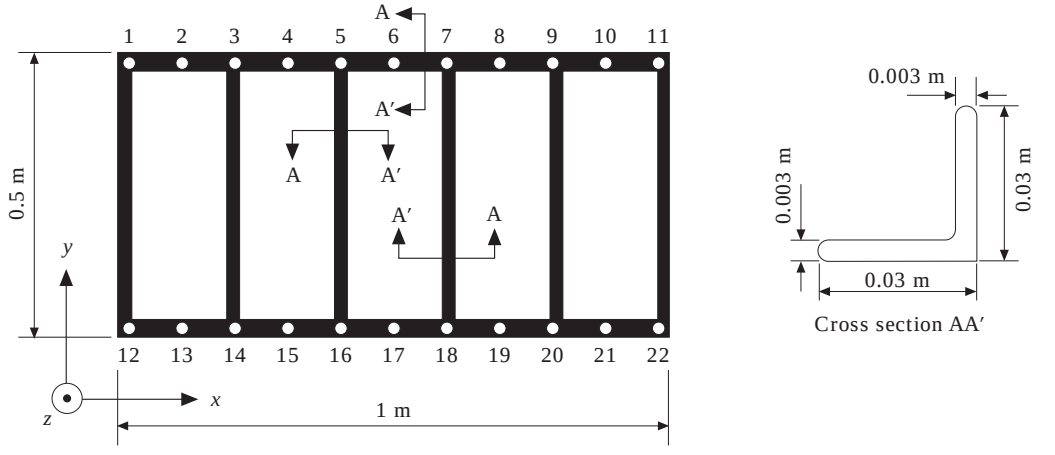

Figure 2. A frame structure as specimen.

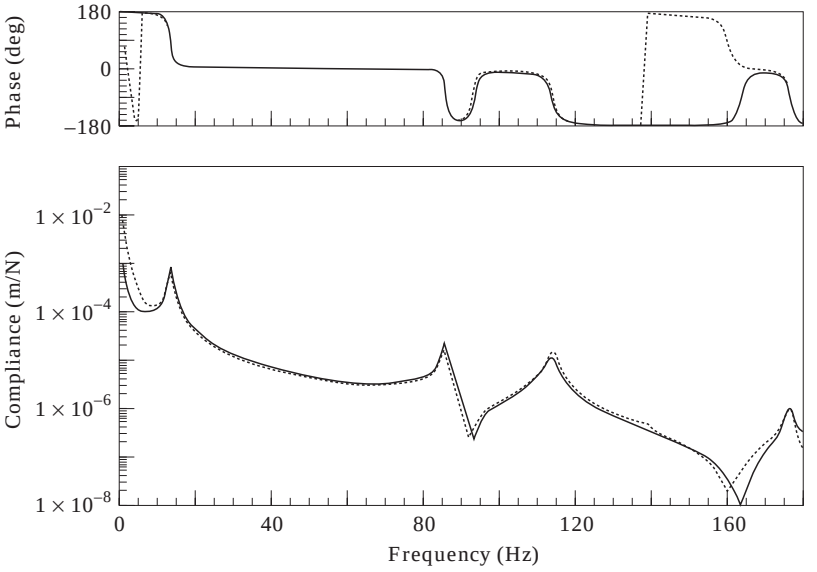

Figure 3. Fitting of FRFs by the identification: ——, identified; ·····, experimental.

results. In the figure, the solid line denotes one of the predicted FRFs of the structure under the clamping, and the dotted line represents the counterpart of the experimentally measured FRFs. The resonant frequencies located in the identification frequency range are observed at about 12, 20, 90 and 112 Hz on the experimental FRFs. On the other hand, Table 2 lists all natural frequencies calculated with the spatial matrices. It is successfully demonstrated that rigid body natural motion modes disappear under clamped boundary condition, and the lowest four natural frequencies are consistent with the experimental ones. All residual natural frequencies successfully move to higher frequencies above the

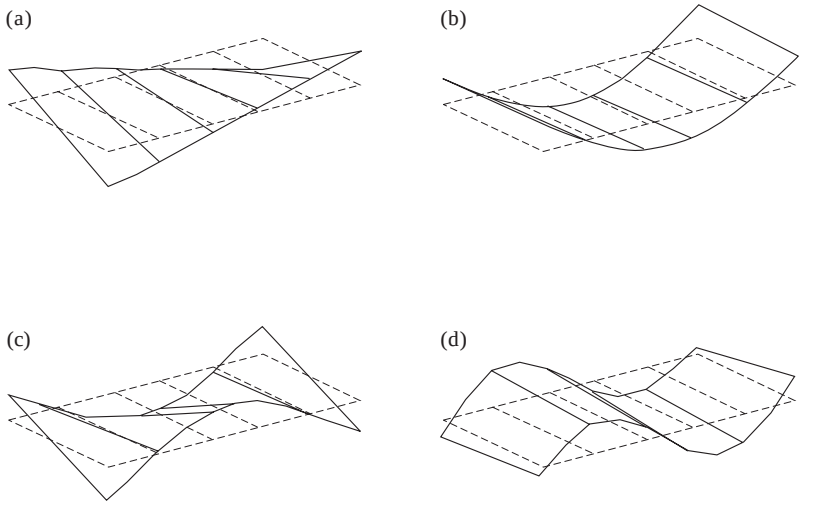

Figure 4. Mode shape orders: (a) first; (b) second; (c) third; (d) fourth.

TABLE 1

Natural frequencies and modal damping ratios calculated from identified matrices

Order	Natural freq. (Hz)	Damping ratios	Order	Natural freq. (Hz)	Damping ratios
1	0·0	0·0	12	477·3	0·0453
2	0·0	0·0	13	494·9	0·0416
3	0·0	0·0	14	523·0	0·0532
4	13·8	0·0288	15	535·1	0·0475
5	86·4	0·0071	16	566·5	0·0609
6	114·0	0·0126	17	586·8	0·0643
7	176·6	0·0048	18	594·7	0·0605
8	223·5	0·0348	19	618·1	0·0676
9	281·6	0·0211	20	626·8	0·0706
10	400·3	0·0451	21	674·8	0·0704
11	447·1	0·0393	22	737·1	0·0696

frequency range. Figure 7 shows the natural modes calculated with the spatial matrices for the frequency range of interest. These are the first bending mode, the first torsional mode, the second bending mode, and the second torsional mode in ascending frequency order. It is experimentally verified that this order is correct. It is noticed here that the change of the orders of the torsional mode and bending mode of the structure under the clamping condition is correctly predicted.

It is already well known that if spatial matrices are identified experimentally, various kinds of experimentally based structural analyses, such as analysis of structural modification, optimum design, simulations integrated with the finite

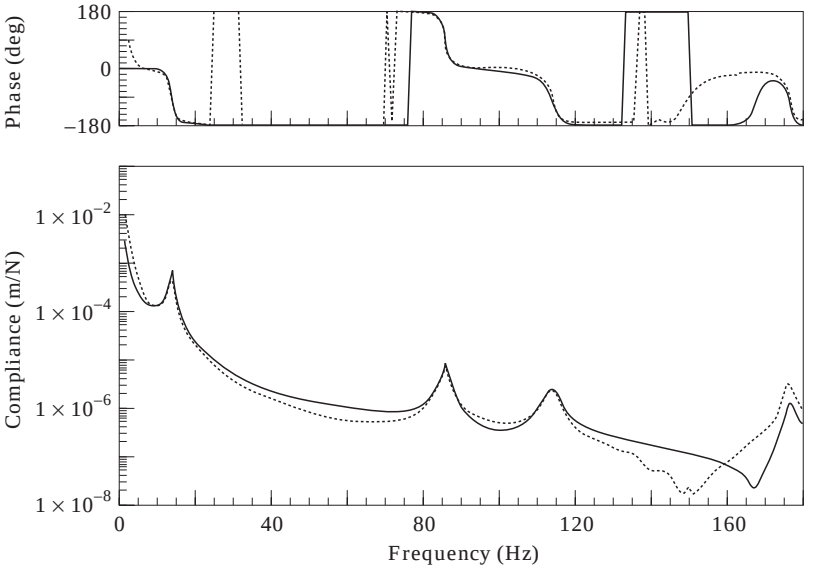

Figure 5. Predicted FRFs of structure excited at another point (driving point: 11, response point: 14). Key as for Figure 3.

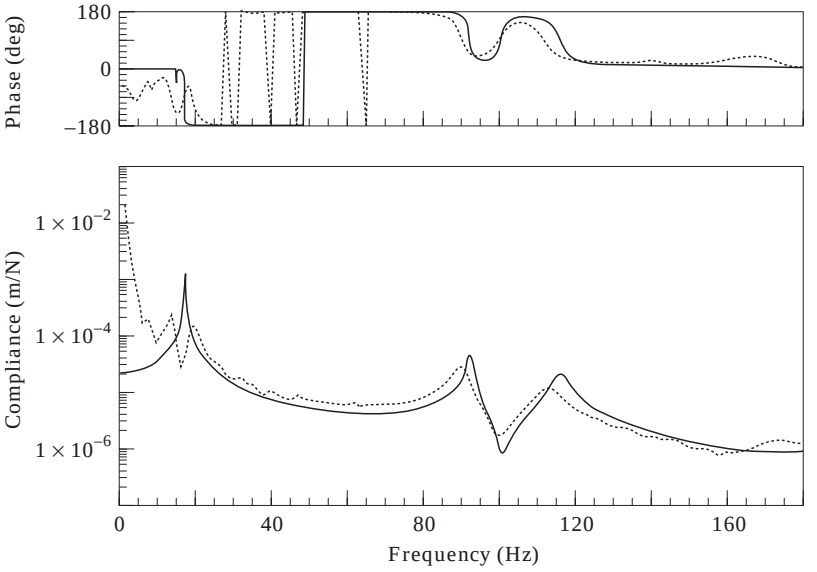

Figure 6. Predicted FRFs of structure under a different boundary condition (driving point: 1, response point: 7). Key as for Figure 3.

element method, vibration control design, etc., may be performed in a much simpler manner. However, if one tries to predict the dynamics of the structure under the clamping boundary condition by using the modal parameters identified under the free–free boundary condition by experimental modal analysis, one has to measure FRFs by changing excitation locations at a minimum of three different points in order to estimate the three feasible natural rigid body motion modes from three sets of inertia terms identified together with the modal parameters of these four resonances [10]. The predictions based on the analysis in the modal domain could not be successfully performed using only modal parameters of these four resonances in the identification frequency range. In the case of this application,

TABLE 2

Predicted natural frequencies and modal damping ratios of structure under a different boundary condition

Order	Natural freq. (Hz)	Damping ratios	Order	Natural freq. (Hz)	Damping ratios
1	15·1	0·0424	10	478·8	0·0503
2	17·5	0·0092	11	508·6	0·0541
3	92·8	0·0048	12	520·3	0·0633
4	116·2	0·0084	13	578·1	0·0610
5	188·7	0·0197	14	585·7	0·0418
6	265·8	0·0059	15	603·5	0·0696
7	290·2	0·0257	16	621·2	0·0701
8	418·8	0·0421	17	667·7	0·0697
9	444·5	0·0465	18	736·8	0·0644

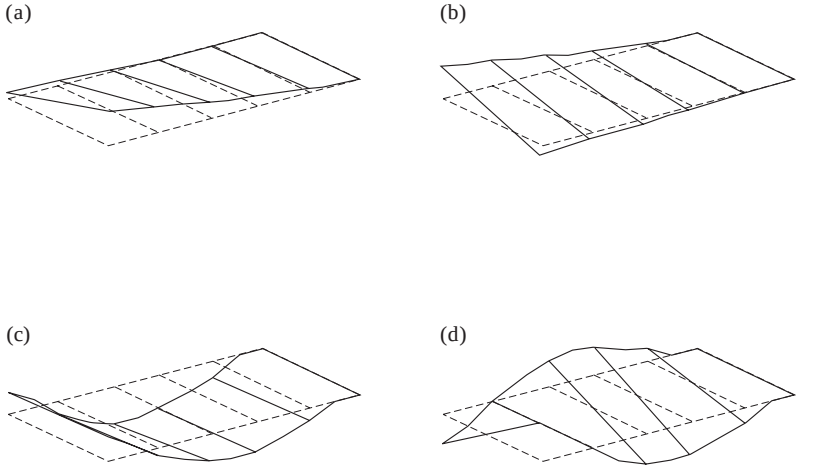

Figure 7. Mode shape orders under clamping four points. Key as for Figure 4.

in which only experimental FRFs under a single point excitation at the measurement point 1 are used, the proposed method obtains successful results, but the prediction analysis in the modal domain does not. These results are compared in Figure 8. In this figure, the dark dotted line expresses the experimental FRF, the light dotted line represents the result of the present method, and the solid line denotes the FRFs predicted by the analysis in the modal domain.

The rigid body properties can also be calculated from the identified mass matrices. Table 3 lists the rigid body properties obtained from the identified mass matrix and the results by other means. The values of the principal inertia of moments in the Measurement column are obtained by the hammering tests as

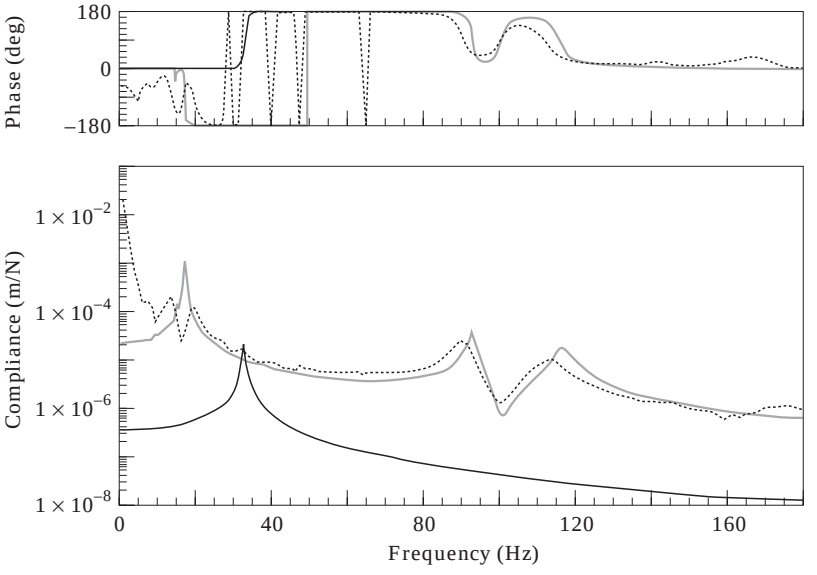

Figure 8. Predicted FRFs of structure under a different boundary condition by modal analysis. Key: ——, modal analysis; · · ·, present method; ——, experiment.

TABLE 3

Rigid body properties

	From the mass matrix	Measurement	Approximate by hand calculation
Mass (kg)	6·6	6·5	6·7
Center of gravity (m)	$X_g = 0{\cdot}466$	0·482	0·490
	$Y_g = 0{\cdot}242$	0·244	0·240
	$Z_g = 0{\cdot}0$	0·0	0·0
Principal moments of inertia (kgm^2)	$I_1 = 0{\cdot}3741$	$0{\cdot}26 \pm 0{\cdot}07$	0·24
	$I_2 = 0{\cdot}7094$	$0{\cdot}82 \pm 0{\cdot}15$	0·63
	$I_3 = 0{\cdot}0$	0·0	0·0
Principal moments of axes of inertia		Assumed as	Assumed as
	I_1-axis (−0·99, 0·013, 0·0)	(1, 0, 0)	(1, 0, 0)
	I_2-axis (−0·013, −0·99, 0·0)	(0, 1, 0)	(0, 1, 0)
	I_3-axis (0·0, 0·0, 1·0)	(0, 0, 1)	(0, 0, 1)

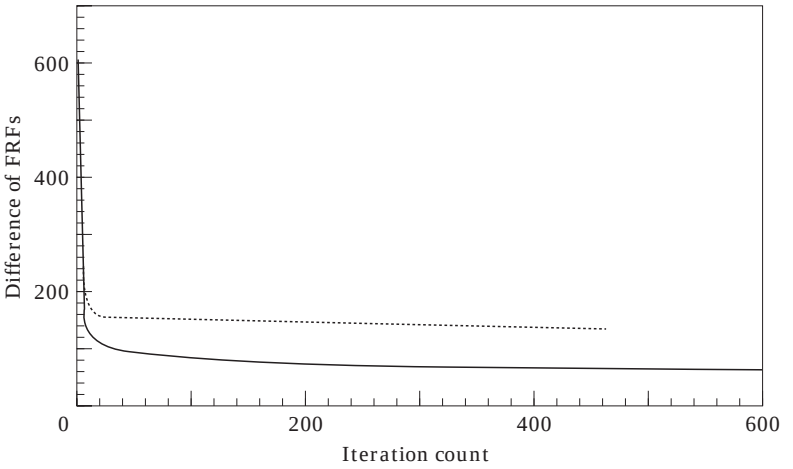

Figure 9. Convergence of fitness of FRFs in "the second improvement". Key: ——, proposed method; · · ·, orthodox method.

follows. The structure is suspended from two strings connected to two points on an assumed principal axis of the moment of inertia. The structure is hit at a point away from the principal axis with a vibration testing hammer, and the acceleration at this point is measured in a rotational manner around the axis by a small accelerometer. The principal moment of inertia is estimated from the applied force and the acceleration and distance of the stricken point using a primitive calculation based on Newton's Second Law. The values listed in the right column are obtained by a simple calculation with the standardized material constants of steel and the specifications of the structural size. Considering that the FRFs are measured by hammering tests, one can conclude that the mass matrix is well identified due to the acceptable accuracy of the rigid body properties regarding the matrix.

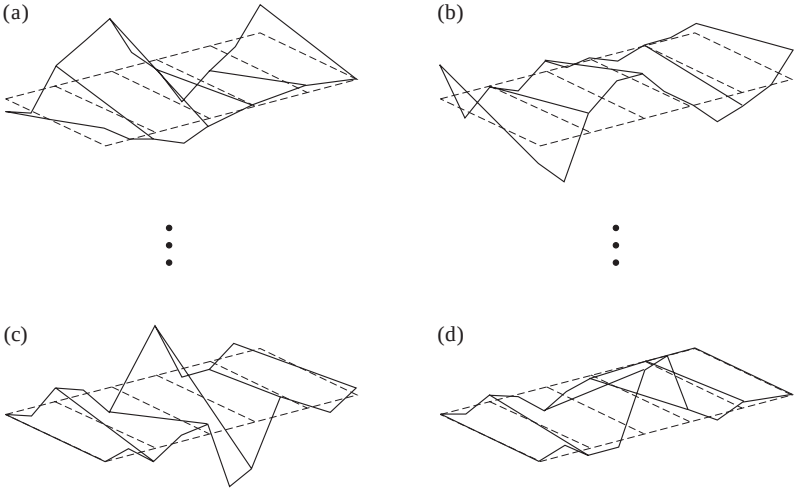

Figure 10. Some of mode shapes of residual orders (order nos. correspond with those of Table 1). Key: (a) eighth; (b) ninth; (c) 21st; (d) 22nd.

Finally, the convergence of the objective function in equation (20) is investigated. Figure 9 shows the comparison of the modified and orthodox steepest descent methods. The solid line denotes the convergence of the steepest descent method modified in this paper as stated in section 2, and the dotted line expresses the convergence of the orthodox steepest descent method. From the figure, it is clear that the proposed modification improves the convergence.

One can summarize the experimental application as follows. Spatial matrices identified by the proposed method are available for such applications as structural analysis, modification and optimum design, and vibration control design. However, it should again be pointed out that the identified spatial matrices may not constitute a unique solution, since they fail to represent realistic natural vibration modes of the residual orders, as depicted in Figure 10. Further investigations will be needed to address this problem.

4. CONCLUSIONS

The authors have presented the current theoretical basis for their experimental spatial matrix identification method. The method can be used to identify the spatial matrices under two necessary conditions: (1) It must be possible to set the number of degrees of freedom of spatial matrices at a value much larger than the number of resonant frequencies located inside the frequency range of interest. (2) The spatial matrices identified must be able to represent the dynamic characteristics of the structure under arbitrary boundary conditions, even conditions that differ from those in place at the time of the identification. The method is then verified through its application to an actual frame structure, and relevant investigations are discussed. Finally, a remaining shortcoming of the method, which should be addressed in future investigations, is described.

REFERENCES

1. H. Vold, J. Kundrat, G. T. Rocklin and R. Russel 1982 *SAE Paper*, 820194. A multi-input modal estimation algorithm for multi-computers.
2. J. M. Leuridan, D. L. Brown, and R. J. Allemang 1982 *AIAA*-82-0767-*CP*, 497. Direct system parameter identification of mechanical structure with application to modal analysis.
3. M. J. Roemer and D. J. Mook 1990 *Proceedings of the Eighth IMAC*. Robust time-domain identification of mass, stiffness and damping matrices.
4. C. Minas and D. J. Inman 1991 *Transactions of ASME*, *Journal of Vibration and Acoustics* **133**, 219–224. Identification of a nonproportional damping matrix from incomplete modal information.
5. L. D. Peterson 1992 *Proceedings of the Tenth IMAC*. Efficient computation of the eigensystem realization algorithm.
6. M. Okuma, T. Ohara, K. Nagao and A. Nagamatsu 1989 *SAE paper*, 891139, 131–138. Application of a new experimental identification method to an engine rigid mount system.
7. M. Okuma and R. Momose 1997 *Transactions of JSME* **63** (616), 4166–4170 Estimation of modal damping ratios from mode indicator functions (in Japanese).

8. R. L. Fox and M. P. Kapoor 1968 *AIAA Journal* **6**, 2426–2477. Rates of change of eigenvalues and eigenvectors.
9. M. Okuma, M. Yamaguchi and A. Nagamatsu 1989 *Proceedings of the ASME PVP Conference* **179**, 57–77. Practical and realistic weighting function for modal curve fitting.
10. M. Okuma and Q. Shi 1997 *Transactions of ASME*, *Journal of Vibration and Acoustics* **119**, 341–345. Identification of the principal rigid body modes under free–free boundary condition.